

# Extensive Air Shower Radio Detection: Recent Results and Outlook<sup>1</sup>

Jonathan L. Rosner and Denis A. Suprun

*Enrico Fermi Institute and Department of Physics  
University of Chicago, Chicago, IL 60637 USA*

**Abstract.** A prototype system for detecting radio pulses associated with extensive cosmic ray air showers is described. Sensitivity is compared with that in previous experiments, and lessons are noted for future studies.

## I INTRODUCTION

The observation of the radio-frequency (RF) pulse associated with extensive air showers of cosmic rays has had a long and checkered history. In the present report we describe an attempt to observe such a pulse in conjunction with the Chicago Air Shower Array (CASA) and Michigan Muon Array (MIA) at Dugway, Utah. Only upper limits on a signal have been obtained at present, though we are still processing data and establishing calibrations.

In Section 2 we review the motivation and history of RF pulse detection. Section 3 is devoted to the work at CASA/MIA, while Section 4 deals with some future possibilities, including ones associated with the planned Pierre Auger observatory. We conclude in Section 5. This report is an abbreviated version of a longer one now in preparation [1].

## II MOTIVATION AND HISTORY

### A Auxiliary information on shower

Present methods for the detection of an extensive air shower of cosmic rays leave gaps in our information. The height above ground at which showers develop cannot be provided by ground arrays, though stereo detection by air fluorescence detectors

---

<sup>1)</sup> Invited talk presented by J. Rosner at RADHEP-2000 Conference, UCLA, Nov. 16–18, 2000, proceedings to be published by AIP. Enrico Fermi Institute Report No. EFI 2000-57, astro-ph/0101089.

is useful. Composition of the primary particles, another unknown, is correlated with shower height, with heavy primaries leading to showers which begin higher in the atmosphere.

Radio detection can help fill such gaps. The electric field associated with a charge  $|e|$  undergoing an apparent angular acceleration  $\ddot{\theta}$  is  $|\mathcal{E}| = 1.5 \times 10^{-26} \ddot{\theta} \text{ V/m}$ , where time is measured in seconds [2,3]. For typical showers the charges of radiating particles are expected to be able to act coherently to give a pulse with maximum frequency component  $\nu_{\max}(\text{MHz}) \simeq 10^6 / R^2(\text{m})$ , where  $R$  is the distance of closest approach of the shower axis to the antenna. Showers originating higher in the atmosphere are expected to have higher-frequency components. Thus RF detection may be able to add information on shower height and primary composition, and to provide a low-cost auxiliary system in projects such as the Pierre Auger array [4].

## B Pulse generation mechanisms

Several possibilities have been discussed for generation of a pulse by air showers. Cosmic rays could induce the atmosphere to act as a giant spark chamber, triggering discharges of the ambient field gradient [5]. Compton scattering and knock-on electrons can give rise to a negative charge excess of some 10 to 25% at shower maximum [6]. Separation of positive and negative charges can occur in the Earth's magnetic field as a result of a  $qv \times \mathbf{B}$  force [7]. This is thought to be the dominant mechanism accounting for pulses with frequencies in the 30 – 100 MHz range [2], and will be taken as the model for the signal for which the search was undertaken. The charge-excess mechanism is probably the major source of an RF signal in a dense material such as polar ice [8], but is expected to be less important in the atmosphere.

## C Early measurements

The first claim for detection of the charge-separation mechanism utilized narrow-band techniques at 44 and 70 MHz [9,10]. A Soviet group reported signals at 30 MHz [11], while a University of Michigan group at the BASJE Cosmic Ray Station on Mt. Chacaltaya, Bolivia [12] studied pulses in the 40–90 MHz range.

The collaboration of H. R. Allan *et al.* [2] at Haverah Park in England studied the dependence of signals on primary energy  $E_p$ , perpendicular distance  $R$  of closest approach of the shower core, zenith angle  $\theta$ , and angle  $\alpha$  between the shower axis and the magnetic field vector. Their results indicated that the electric field strength per unit of frequency,  $\mathcal{E}_\nu$ , could be expressed as

$$\mathcal{E}_\nu = s \frac{E_p}{10^{17} \text{ eV}} \sin \alpha \cos \theta \exp \left( -\frac{R}{R_0(\nu, \theta)} \right) \quad \mu\text{V} \text{ m}^{-1} \text{ MHz}^{-1} \quad , \quad (1)$$

where  $R_0$  is an increasing function of  $\theta$ , equal (for example) to  $(110 \pm 10)$  m for  $\nu = 55$  MHz and  $\theta < 35^\circ$ . The constant  $s$  was originally claimed to be 20. The

Haverah Park observations were recalibrated to yield  $s = 1.6$  ( $0.6 \mu\text{V m}^{-1} \text{MHz}^{-1}$  for a  $10^{17}$  eV shower at  $R = 100$  m) while observations in the U.S.S.R. gave  $s = 9.2$  ( $3.4 \mu\text{V m}^{-1} \text{MHz}^{-1}$  at  $R = 100$  m) [13]. To estimate the corresponding signal strength in [9,10], we note that the signal power for showers of average primary energy  $E = 5 \times 10^{16}$  eV was measured to be about 4 times that of galactic noise, for which [2]  $\mathcal{E}_\nu^{\text{Gal}} \simeq 1\text{--}2 \mu\text{V m}^{-1} \text{MHz}^{-1}$ . Thus, for such showers, one expects  $\mathcal{E}_\nu \simeq 2\text{--}4 \mu\text{V m}^{-1} \text{MHz}^{-1}$ . Similarly, the estimate [10] of an average pulse power  $V_{\text{peak}}^2/2R = 10^{-12}$  W gives  $V_{\text{peak}} = 10 \mu\text{V}$  for  $R = 50 \Omega$ . Using the relation between pulse voltage and  $\mathcal{E}_\nu$  [2]

$$V = 30G^{1/2}(\delta\nu/\nu)\mathcal{E}_\nu \quad , \quad (2)$$

where  $G$  is the antenna gain, and  $\delta\nu$  is the bandwidth centered at frequency  $\nu$ , we find for  $G = 5$  (7 dB) and  $\delta\nu/\nu = 2.75/44$  [9], a value of  $\mathcal{E}_\nu \simeq 2.4 \mu\text{V m}^{-1} \text{MHz}^{-1}$  at a primary energy of  $5 \times 10^{16}$  eV, or about  $5 \mu\text{V m}^{-1} \text{MHz}^{-1}$  at  $10^{17}$  eV if  $\mathcal{E}_\nu$  scales linearly with primary energy [2]. The data of Refs. [9,10] thus favor the higher field-strength claims of the U.S.S.R. group cited in Ref. [13].

More recent claims include pulses with components at or below several MHz [15–18], and at VHF frequencies [17,18]. The Gauhati University group has reviewed evidence for pulses at a wide range of frequencies [18].

## D Pulse characteristics

The Haverah Park observations are consistent with a model in which the pulse's onset is generated by the start of the shower at an elevation of about 10 km above sea level, while its end is associated with the greater total path length (shower + signal propagation distance) associated with the shower's absorption about 5 km above sea level. If a vertical shower is observed at a distance of 100 m from its core, the pulse should rise and fall back to zero within about 10 ns, with a subsequent longer-lasting negative component. High frequencies should be less visible far from the shower axis. Heavy primaries should lead to showers originating higher in the atmosphere, with consequent higher-frequency RF components as a result of the geometric aspect ratio with which they are viewed by the antenna, and possibly a greater  $\mathcal{E}_\nu$  for a given primary energy [2]. The polarization of the pulse should be dictated by the mechanism of pulse generation: e.g., perpendicular to the line of sight with component along  $\mathbf{v} \times \mathbf{B}$  for the charge-separation mechanism.

## E RF backgrounds

Discharges of atmospheric electricity will be detected at random intervals at a rate depending on local weather conditions and ionospheric reflections. Man-made RF sources include television and radio stations, police and other communications

services, broad-band sources (such as ignition noise), and sources within the experiment itself. The propagation of distant noise sources to the receiver is a strong function of frequency and of solar activity.

Galactic noise can be the dominant signal in exceptionally radio-quiet environments for frequencies in the low VHF (30–100 MHz) range [2]. For higher frequencies in such environments, thermal receiver noise becomes the dominant effect.

### III THE INSTALLATION AT CASA

The CASA/MIA detector is located about 100 km southwest of Salt Lake City, Utah, at the Dugway Proving Ground, in the midst of the Fly’s Eye II array [14]. The Chicago Air Shower Array (CASA) [14] is a rectangular grid of  $33 \times 33$  stations on the desert’s surface. The inter-station spacing is 15 m. A station has four  $61 \text{ cm} \times 61 \text{ cm} \times 1.27 \text{ cm}$  sheets of plastic scintillator each viewed by its own photomultiplier tube (PMT). When a signal appears on 3 of 4 PMTs in a station, a “trigger request pulse” of 5 mA with  $5 \mu\text{s}$  duration is sent to a central trailer, where a decision is made on whether to interrogate all stations for a possible event. Details of this trigger are described in Ref. [14]. When this experiment was begun the CASA array had been reconfigured to remove the 4 westernmost “ribs” of the array. For runs performed in 1998, the easternmost rib had also been removed.

The University of Michigan designed and built a muon detection array (MIA) to operate in conjunction with CASA. It consists of sixteen “patches,” each having 64 muon counters, buried 3 m below ground at various locations in the CASA array. Each counter has lateral dimensions  $1.9 \text{ m} \times 1.3 \text{ m}$ . Four of the patches (numbered 1 through 4), each about 45 m from the center of the array, lie on the corners of a skewed rectangle; four (numbered 5 through 8), each about 110 m from the center of the array, lie on a rectangle with slightly different skewed orientation, and eight (numbered 9 through 16) lie on the sides and corners of a rectangle with sides  $x \simeq \pm 180 \text{ m}$  and  $y \simeq \pm 185 \text{ m}$ , where  $x$  and  $y$  denote East and North coordinates.

### A Expected integral rates

The CASA trigger threshold is a few  $\times 10^{14}$  eV and corresponds to a trigger rate of 10–20 Hz. The expected rates above ( $10^{15}$ ,  $10^{16}$ ,  $10^{17}$ ,  $10^{18}$ ) eV are about (1 Hz, 1 per 2 min, 1 per 4 hr, and 2 per mo), respectively, over the  $1/4 \text{ km}^2$  area of the array. A primary energy of at least  $10^{17}$  eV seems to be needed if radio signals are to exceed the galactic noise level of  $1\text{--}2 \mu\text{V m}^{-1} \text{ MHz}^{-1}$ . Such pulses could be generated by a  $10^{17}$  eV vertical shower with axis 100 m from the antenna under the most optimistic estimates. Since the whole array should see such showers only every few hours, and most have axes farther from the antenna than 100 m, the possibility of accidental noise pulses during such long time intervals reduces the expected sensitivity considerably.

## B The “radio shack” at CASA

A survey of the CASA/MIA site determined that within the array, broad-band noise associated with computers, switching power supplies, and other electronics was so intense that no RF searches could be undertaken. The same was true at any position within the perimeter of the array. Consequently, an antenna was mounted at on top of a mobile searchlight tower at a height of 10 m about 24 m east of the array, corresponding to  $x = 263.8$  m,  $y = 0$  m. The antenna, a 9-element portable log-periodic antenna manufactured by Dorne and Margolin, was acquired from FairRadio Co. in Lima, Ohio, for about \$60. Its nominal bandwidth is 26–76 MHz but it was measured to have usable properties up to 170 MHz.

The signal was fed into a trailer located about 10 m closer to the array, and preamplified using either one or two MiniCircuits ZFL-500LN preamplifiers, each with 26 dB of gain. Filters by Minicircuits were used to define a bandpass. The “wide-band” configuration used for most data acquisition runs consisted of a high-pass filter admitting frequencies above 23 MHz, one preamplifier, and a low-pass filter admitting frequencies below 250 MHz. A “narrow-band” configuration with response between 23 and 37 MHz and two preamplifiers had substantially poorer signal-to-noise ratio in distinguishing transient signals from background.

A trigger based on the coincidence of seven of the eight outer muon “patches” was set to select large showers. Each muon patch was set to produce a trigger pulse when at least 5 of its 64 counters registered a minimum-ionizing pulse within 5.2  $\mu$ s of one another. The pulses were then combined to produce a summed pulse, fed to a discriminator, whose output was amplified and sent over a cable (with measured delay time 2.15  $\mu$ s) to the RF trailer. No evidence for pickup of the trigger pulse from the antenna was found. The trigger corresponded to a minimum shower energy somewhat below  $10^{16}$  eV, based on the integral rate [19] at  $10^{18}$  eV of 0.15/km<sup>2</sup>/day/sr.

A Tektronix TDS-540B digitizing oscilloscope registered filtered and preamplified RF data on a rolling basis. These data were then captured upon receipt of a large-event trigger and stored on hard disk using a National Instruments GPIB interface. Data were taken using separate computers (at different times), allowing for analysis both at the University of Washington and at Chicago. The Washington system used a Macintosh Quadra 950 running Labview, while the Chicago system used either a Dell XPS200s Pentium desktop computer or a Dell Latitude LM laptop computer running a C program adapted from those provided by National Instruments. Each trigger caused 50  $\mu$ s of RF data, centered around the trigger and acquired at 1 GSa/s, to be saved.

The total trigger rate ranged between about 20 and 50 events per hour, depending on intermittent noise sources in the trigger system. Concurrently, the CASA on-line data acquisition system was instructed to write files of events in which at least 7 out of the 8 outermost muon patches produced a patch pulse. These files typically overlapped with the records taken at the RF trailer to a good but not perfect extent as a result of occasional noise on the trigger line.

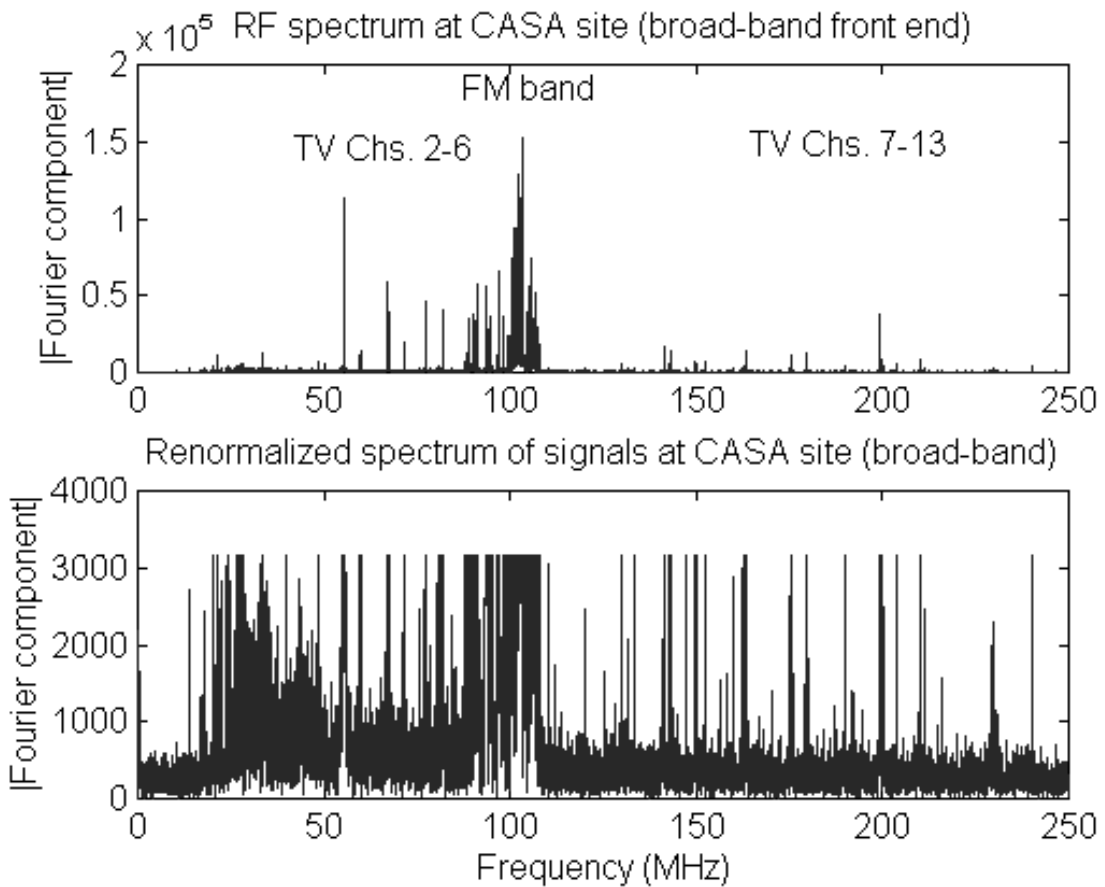


**FIGURE 1.** Top panel: Fourier spectrum (in arbitrary units) of RF signals at Dugway site. Prominent features include video and audio carriers for TV Channels 2, 4, 5, 7, and 11, and the FM broadcast band between 88 and 108 MHz. Bottom panel: Fourier spectrum (same vertical scale) after renormalization of large Fourier components to an arbitrary maximum magnitude. The continuum between 23 and 88 MHz is not detectable in a city environment; TV and FM signals were found to be almost 40 dB stronger at the University of Chicago.

### C Raw data and RF backgrounds

To remove strong Fourier components associated with narrow-band RF signals which were approximately constant over the duration of each data record, a MATLAB routine performed the fast Fourier transform of the signal and renormalized the large Fourier components to a given maximum intensity. Fig. 1 shows the fast Fourier transform of a typical RF signal before and after this procedure was applied. In each case the data were acquired using the “wide-band” filter configuration mentioned above, whose response cuts off sharply below 23 MHz.

The effect of digital filtering on detectability of a transient is illustrated in Fig. 2. The top panel shows the RF record whose Fourier transform was given in Fig. 1, on which has been superposed a simulated transient of peak amplitude 14.5 digitization

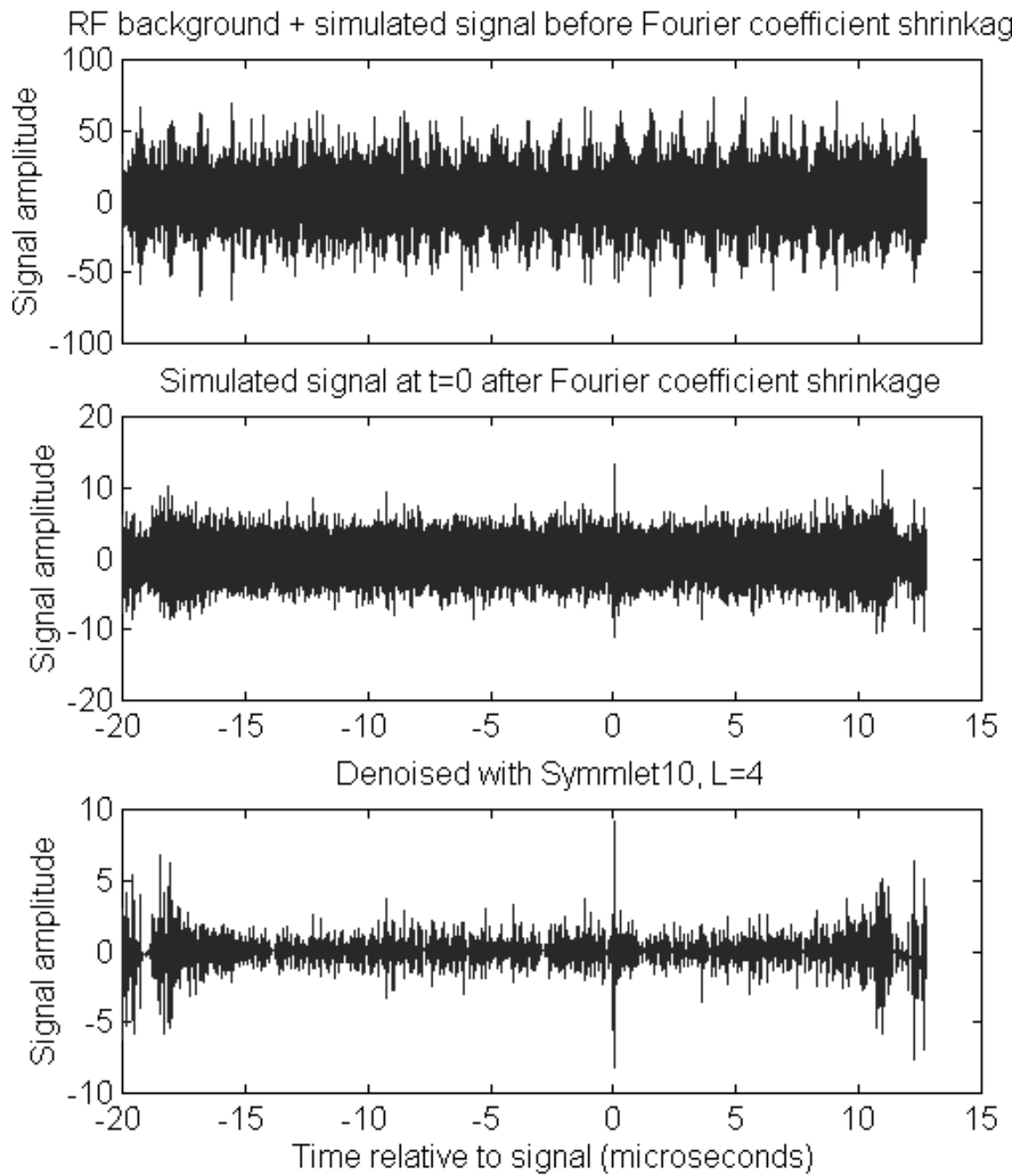


**FIGURE 2.** Effect of Fourier coefficient shrinkage on detectability of a transient. Top panel: raw RF record (in arbitrary units) with simulated signal superposed. Middle panel: record (same scale) after Fourier coefficient shrinkage. Here a maximum Fourier coefficient magnitude of  $10^3$  (in the units of Fig. 1) has been imposed. Bottom panel: the same record after denoising with a wavelet routine.

units. (The data acquisition scale ranges from  $-128$  to  $+127$  digitization units; one scale division on the oscilloscope corresponds to 25 units.) The transient is invisible beneath the large amplitude associated with television and FM radio signals. The middle panel shows the result after application of the Fourier coefficient shrinkage algorithm. The bottom panel shows the same record after denoising with a wavelet routine [21]. The records in Figs. 1 and 2 were obtained for 32,768 data points obtained at a 1 ns sampling interval, with the trigger at the 20,000th point.

## D Signal simulation

To quantify signal processing efficiency, we generated the expected signal, fed it through the same preamplifier and filter configurations used for data acquisition, and superposed it on records otherwise free of transients. We successively reduced the amplitude of the superposed test signal until it was no longer detectable, thereby obtaining an estimate of sensitivity.

A Hewlett-Packard Arbitrary Waveform Generator was used to generate signals whose typical characteristics are illustrated in Fig. 3. These signals were taken to have the form  $f(t) = \theta(t)At^2(e^{-Bt} - Ce^{-Dt})$  with the coefficient  $C$  chosen so that  $f(t)$  has no DC component, and  $D$  corresponding to a long duration of the negative-amplitude component. For all pulses we chose  $D = B/20$ , so that  $C = (8000)^{-1}$  cancels the DC component. The Fourier components of the test pulse fall off smoothly with frequency. The initial  $t^2$  behavior was chosen so that both the test pulse and its first derivative vanish at  $t = 0$ , as might be expected for a pulse from a developing shower. We chose  $B = 0.8, 0.4, 0.2, 0.1$  corresponding to  $\delta = 2.5, 5, 10, 20$  ns and simulated both narrow-band (23–37 MHz) and broad-band (23–250 MHz) configurations.

The shape of the pulse of Fig. 3 is affected by preamplification and filtration as shown in Fig. 4 for the broad-band example. (The narrow-band configuration leads to a longer ringing time.) The noise and the sharp feature at 125 MHz are associated with the system used to generate the test pulse, and the fact that the Fourier transform is taken over a much longer time than the duration of the pulse.

Systematic studies of signal-to-noise ratios have been performed so far only for the simulated pulses with  $\delta = 5$  ns applied to the broad-band front end. A typical pulse of this type gave a front end output of 21 mV peak-to-peak, acquired at an oscilloscope sensitivity of 5 mV per division. Since each division corresponds to 25 digitization units, the peak-to-peak range is about 104 digitization units, or slightly less than half the dynamic range (255 units, or 8 bits). Positive and negative peaks are thus about 52 digitization units each.

The stored test signal is then multiplied by a scale factor and added algebraically to a collection of RF records in which, in general, randomly occurring transients will be present. One then inspects these records to see if the transient can be distinguished from random noise.

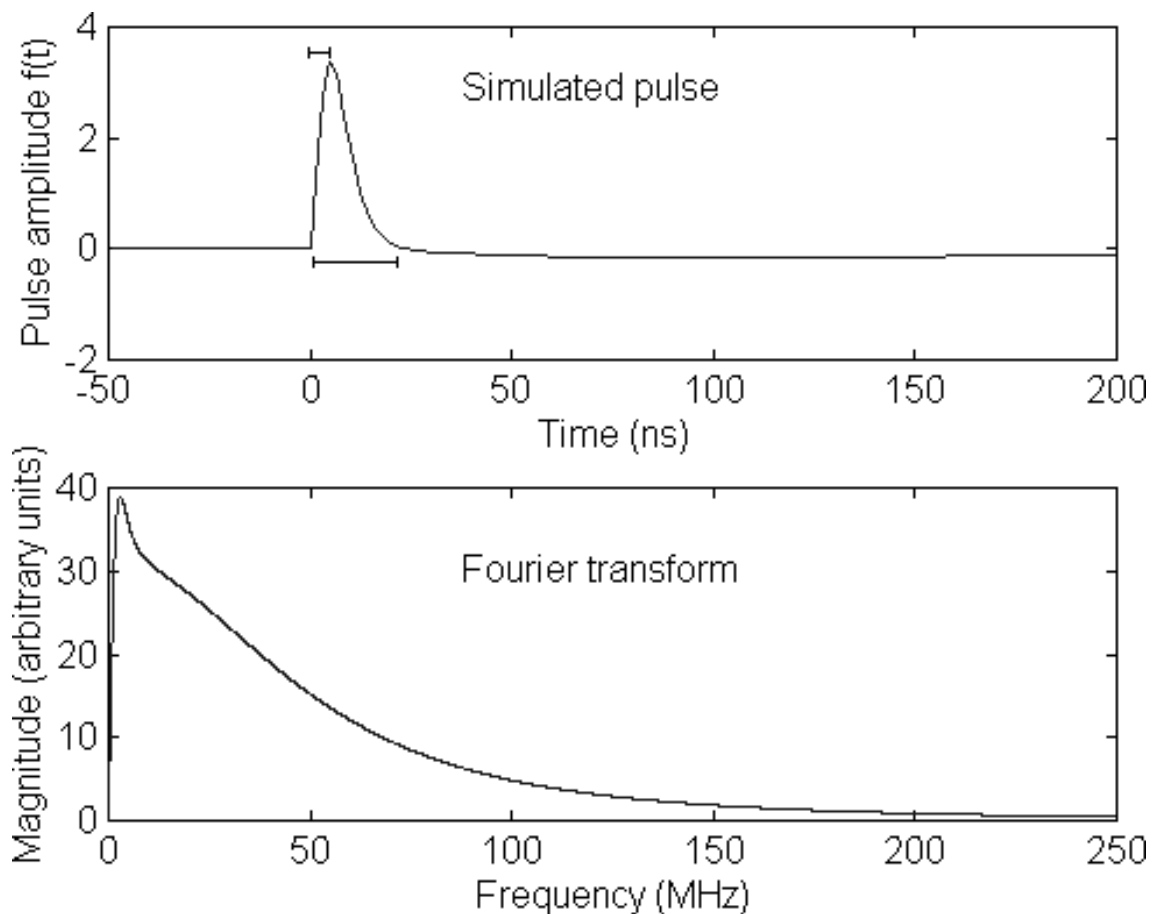


**FIGURE 3.** Analytic depiction of typical pulse presented to filter-preamplifier configuration. Top panel: time dependence of pulse  $f(t) = \theta(t)t^2[e^{-0.4t} - e^{-0.02t}/8000]$  ( $t$  in ns); bottom panel: Fourier spectrum of pulse for  $-20 \mu\text{s} \leq t \leq 12.768 \mu\text{s}$  (calculated analytically). In the top panel,  $\delta$  is the time difference between onset and maximum, while  $\Delta$  is the duration of the positive component of the pulse.

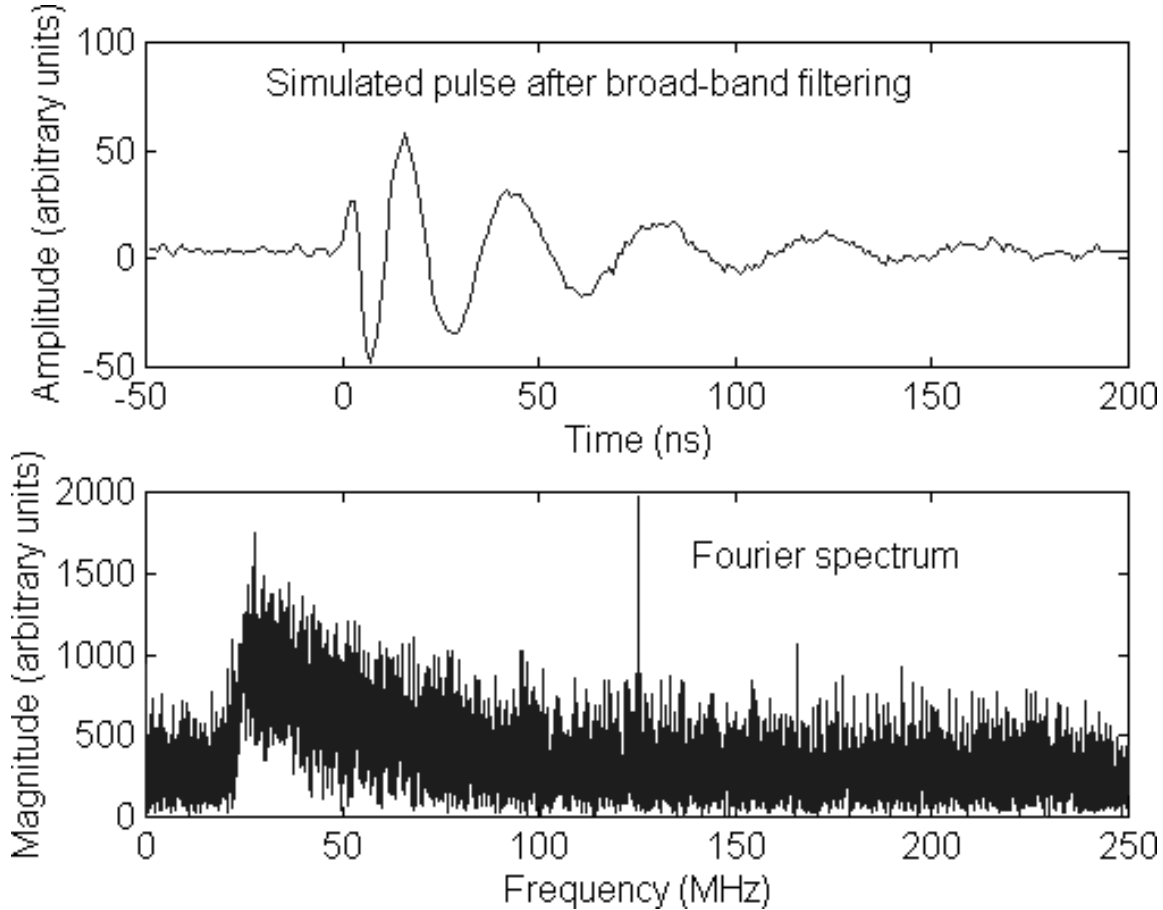


**FIGURE 4.** Test pulse of Fig. 3 after broad-band filtration (23–250 MHz) and preamplification. Top panel: time dependence of pulse; bottom panel: Fourier spectrum of recorded pulse for  $-20\mu\text{s} \leq t \leq 12.768\ \mu\text{s}$ .

For the broad-band data we estimated that pulses with input voltages corresponding to about 1/5 the original test pulse can be distinguished from average noise (not from noise spikes!). Since the original test pulse had a peak value of 1.3 mV, this corresponds to sensitivity to an antenna output of about  $V_{\text{pk}} \simeq 260\mu\text{V}$ . The ability to detect such a pulse with an effective bandwidth of about 30 MHz corresponds to a threshold sensitivity at the level of order  $2\ \mu\text{V/m/MHz}$  [1].

Preliminary studies of simulated pulses applied to the narrow-band front end suggest a considerably poorer achievable signal-to-noise ratio, despite the expectation that the signal should have a large portion of its energy between 23 and 37 MHz. It appears difficult to detect a pulse from the antenna below about 0.7 mV, which for a bandwidth of 10 MHz corresponds to a threshold sensitivity of  $6\ \mu\text{V/m/MHz}$  [1]. Studies of possible improvements of the analysis algorithm for the narrow-band data are continuing.

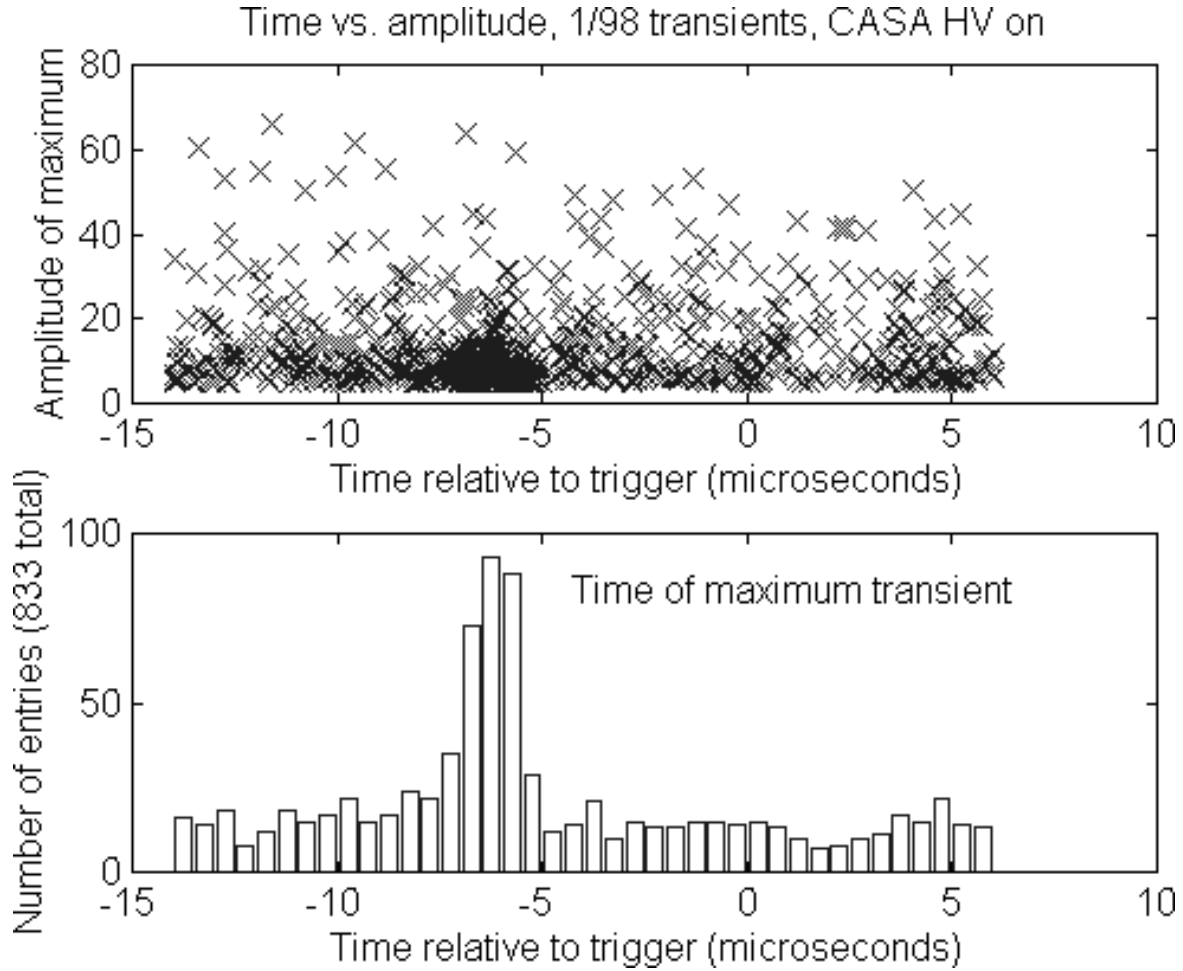


**FIGURE 5.** Top panel: time-vs.-amplitude plot for maxima of 833 events recorded in January 1998 with CASA HV supplied to all stations. All events recorded with East-West antenna polarization. Bottom panel: time distribution of transients.

## E Transients detected under various conditions

Several means were used to characterize transients. One method with good time resolution involved the shrinkage of large Fourier coefficients, followed by a wavelet denoising procedure. One can then search for the maximum of each data record, plotting its amplitude against its time relative to the trigger. One such plot is shown in Fig. 5 for a data run in which CASA HV was delivered to all boxes. A strong accumulation of transients, mostly with amplitude just above the arbitrarily chosen threshold, is visible at times  $-5.5$  to  $-7$   $\mu$ s relative to the trigger. In a comparable plot for a run in which CASA HV was completely disabled (Fig. 6), no such accumulation is visible. This pattern persists through all runs. A typical transient occurring in a run with CASA HV on is shown in Fig. 7. The transients are highly suppressed (though not in all runs) when CASA boxes within 100 m of

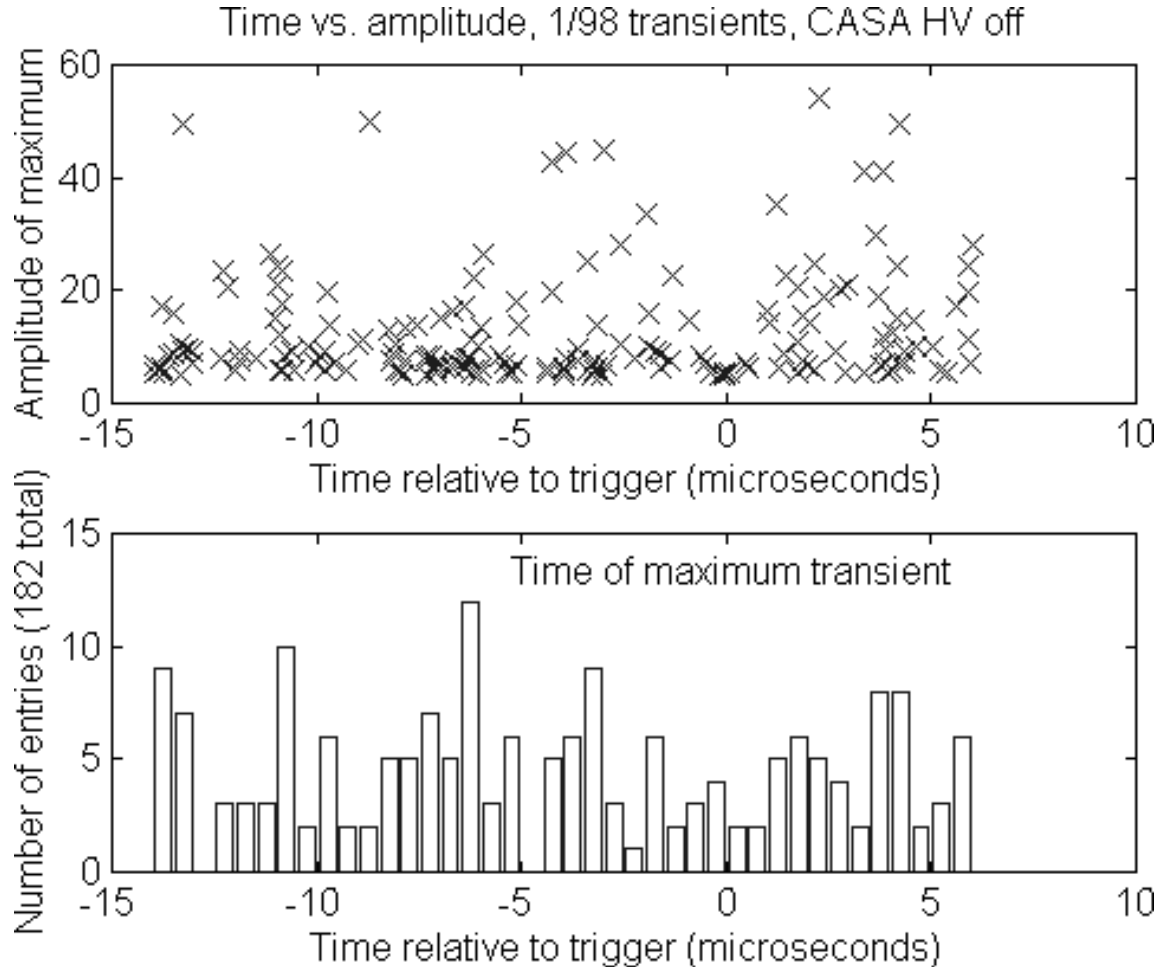


**FIGURE 6.** Top panel: time-vs.-amplitude plot for maxima of 182 events recorded in January 1998 with CASA HV disabled. All events recorded with East-West antenna polarization. Bottom panel: time distribution of transients.

the antenna are disabled.

The time distribution of event maxima above an arbitrary threshold for 833 events taken with CASA HV on (the full sample from January 1998) is shown in the bottom panel of Fig. 5. The mean arrival time is about  $6 \mu\text{s}$  before the trigger, with a distribution which is slightly broader for pulses arriving earlier than the mean. This broadening may correspond to some jitter in forming the trigger pulse from the sum of muon patch pulses.

As mentioned earlier, the time for the trigger pulse to propagate from the central station to the RF trailer was measured to be  $2.15 \mu\text{s}$ . One expects a similar travel time for pulses to arrive from muon patches to the central station. Moreover, the muon patch signals are subjected to delays so that they all arrive at the central station at the same time for a vertically incident shower. Thus, the peak in Fig. 6 is consistent with being associated with the initial detection of a shower by

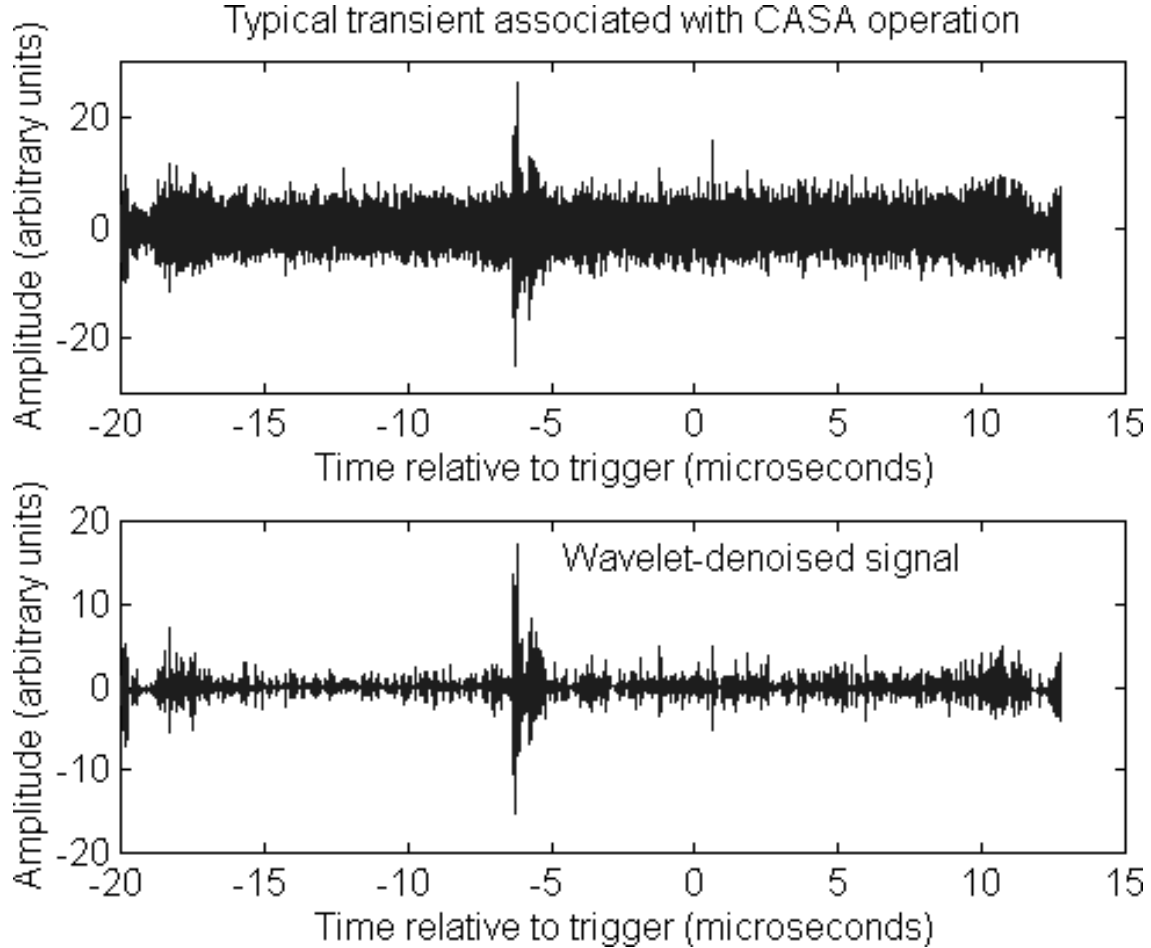


**FIGURE 7.** Signal of a typical transient associated with CASA operation. Top panel: before denoising; bottom panel: after denoising.

CASA boxes. This circumstance was checked by recording CASA trigger request signals simultaneously with other data; they coincide with transients such as those illustrated in Fig. 7 within better than  $1/2 \mu\text{s}$ .

The RF signals from the shower are expected to arrive around the same time as, or at most several hundred nanoseconds before, the transients associated with CASA operation. They would propagate directly from the shower to the antenna, whereas transients from CASA stations are associated with a slightly longer total path length from the shower via the CASA station to the antenna. There will also be some small delay at a CASA station in forming the trigger request pulse. Thus, we expect a genuine signal also to show up around  $6\text{--}7 \mu\text{s}$  before the trigger. However, for data recorded with CASA boxes disabled, no significant peak is visible in this time window. The upper limit on the rate of events giving rise to such a peak can be used to set a limit on RF pulses associated with air showers.

In Table 1 we summarize the triggers taken under optimum conditions, corresponding to broad-band data acquisition under conditions of minimum ambient

**TABLE 1.** Broad-band data recorded under lowest-noise conditions.

Antenna Polarization	CASA HV on	CASA HV off	Partial CASA HV	Total events
East-West	4503	857	1834	7194
North-South	677	641	366	1821
Total events	5180	1498	2200	9015

noise. These triggers represent about 50 hours of data. Data were taken with both East-West and North-South antenna polarizations. Since noise from CASA boxes was found to be a significant source of RF transients, data were taken with some or all CASA boxes disabled by turning off high voltage (HV) supply to the photomultipliers.

## F Sensitivity estimate

The main difficulty associated with pulse detection is that signal pulses are not easily distinguishable from large spurious pulses originating from atmospheric discharges. Both air shower pulses and these background noise pulses can considerably exceed the average noise level. We estimate that all signal pulses should arrive between 7 and 6  $\mu$ s before the trigger, while the time distribution of noise pulses is assumed to be uniform. Hence, a sufficiently large relative accumulation of pulse maxima in that time bin was adopted as a key criterion in search of signal pulses. We also employed several criteria to increase the fraction of signal pulses: The pulse should be larger than some specified magnitude threshold, bandwidth limited and approximately uniform within its limited bandwidth. To date, no significant accumulation has been detected.

At present we are only able, after accounting for the rate of accidental noise pulses and using Monte-Carlo simulation, to set an upper limit of  $s = 46$  in Eq. (1). This is to be compared with the original Haverah Park result  $s = 20$  [2], the recalibrated result  $s = 1.6$  [13], and the Soviet group's result  $s = 9.2$  [13]. The noise level at Dugway is too high and acquired statistics is quite limited to allow us to place upper limits strict enough to check the claims of the two groups. We hope that further improvement of the data processing technique will reduce the noise contribution. The magnetic dip angle  $\gamma$  is much smaller at the Auger site in Argentina ( $34^\circ$  versus  $68^\circ$  at Utah), leading one to expect bigger electric fields for vertical showers and facilitating the detection of shower radiation. We also expect that the Argentina site will be quieter than Dugway and some clarity as regards the calibrating factor will be established.

## IV OUTLOOK

### A Further possibilities for processing present data

We are still hoping to improve our sensitivity to the point that we can see a true RF signal from a shower even when CASA HV is not disabled. Such a signal should precede CASA-related transients by at least the delay of formation of a phototube signal. An important calibration will be achieved if we can determine whether we are sensitive to galactic noise, which may be responsible for the continuum between 23 and 88 MHz visible in Fig. 1.

We are still exploring improved methods for removing constant RF signals from our records. In this respect we are limited by the 8-bit dynamic range of the TDS-540B oscilloscope. Data taken with various configurations of boxes near the antenna disabled may help us to better characterize the CASA-related transients.

The triggered data may be useful in a rather different context. It has been proposed that radar methods be used to detect ion trails associated with extensive air showers [22]. In our case we may be able to investigate sudden enhancements of the signals of distant television signals (on Channels 3, 6, 8, and 12) correlated with receipt of a large-event trigger.

### B Considerations for Auger site

A number of questions have been suggested by the present investigation if RF pulse detection is to be considered as an adjunct to the Auger array.

- How far from the shower axis can antennas detect pulses from showers with energies above  $10^{18}$  or  $10^{19}$  eV? The answer determines whether a sparse array (e.g., one with the same density as Auger stations) would be sensitive to the RF pulse.
- What dynamic range for a data-acquisition system is needed so that a transient signal survives digital filtering? Apparently 8-bit range is not enough.
- What RF interference exists at each site? Surveys would be desirable. They could pinpoint not only narrow-band sources due to broadcasting stations but potentially dangerous broadband sources from switching power supplies, computers, etc. It would be best to undertake such studies after prototype systems are in place.
- What power budget would an RF detection system need? Each Auger solar-powered station is limited to a total budget of 10 watts. Presumably an RF system would have to use auxiliary power, particularly for its fast-digitization and memory components.

- What is the envisioned minimum cost per RF station? It would presumably be dominated by the data-acquisition system; the antennae and preamplifiers would probably be cheap by comparison. A preliminary estimate is less than \$3K per station [1].

The Southern Hemisphere Auger site is progressing well toward an engineering array of 40 stations, as we have heard at this conference [23]. It is hoped that in a couple of years an investigation at that site of the feasibility of RF pulse detection can be undertaken.

## V CONCLUSIONS

No “golden signal” has been seen for an RF transient associated with extensive air showers of cosmic rays at the CASA site. With further processing, the data may permit the setting of useful upper limits on signals relevant to at least some of the previous claims. A number of useful lessons have been learned if a similar technique is to be tried in conjunction with the Auger project.

## VI ACKNOWLEDGEMENTS

It is a pleasure to thank Mike Cassidy, Jim Cronin, Brian Fick, Lucy Fortson, Joe Fowler, Rachel Gall, Kevin Green, Brian Newport, Rene Ong, Scott Oser, Daniel F. Sullivan, Fritz Toebs, Kort Travis, Augustine Urbas, and John Wilkerson for collaboration and support on various aspects of this experiment. Thanks are also due to Bruce Allen, Dave Besson, Maurice Givens, Peter Gorham, Kenny Gross, Dick Gustafson, Gerard Jendraszkiewicz, Larry Jones, Dave Peterson, John Ralston, Leslie Rosenberg, David Saltzberg, Dave Smith, M. Teshima, and Stephan Wegerich for useful discussions. This work was supported in part by the Enrico Fermi Institute, the Louis Block Fund, and the Physics Department of the University of Chicago and in part by the U. S. Department of Energy under Grant No. DE FG02 90ER40560.

## REFERENCES

1. K. Green, J. L. Rosner, D. Suprun, K. Travis, and J. F. Wilkerson, Enrico Fermi Institute Report No. EFI-00-14, article in preparation for submission to *Nucl. Instr. Meth.*
2. H. R. Allan, in *Progress in Elementary Particles and Cosmic Ray Physics*, v. 10, edited by J. G. Wilson and S. G. Wouthuysen (North-Holland, Amsterdam, 1971), p. 171, and references therein.
3. R. P. Feynman, R. B. Leighton, and M. Sands, *The Feynman Lectures in Physics*, Addison-Wesley, Reading, Mass., 1963, Sec. I-28.

4. J. W. Cronin, Rev. Mod. Phys. **71**, S165 (1998); Nucl. Phys. B Proc. Suppl. **80**, 33 (2000); D. Zavrtanik, Nucl. Phys. B Proc. Suppl. **85**, 324 (2000). For the Pierre Auger Project Design Report see <http://www.ses-ng.si/public/pao/design.html>.
5. R. R. Wilson, Phys. Rev. **108**, 155 (1967).
6. G. A. Askar'yan, Zh. Eksp. Teor. Fiz. **41**, 616 (1961) [Sov. Phys.–JETP **14**, 441 (1962)]; Zh. Eksp. Teor. Fiz. **48**, 988 (1965) [Sov. Phys.–JETP **21**, 658 (1965)].
7. F. D. Kahn and I. Lerche, Proc. Roy. Soc. **A 289**, 206 (1966).
8. E. Zas, F. Halzen, and T. Stanev, Phys. Rev. D **45**, 362 (1992).
9. J. V. Jelley *et al.*, Nature **205**, 327 (1965); Nuovo Cimento **A46**, 649 (1966); N. A. Porter *et al.*, Phys. Lett. **19**, 415 (1965).
10. T. Weekes, this conference.
11. S. N. Vernov *et al.*, Pis'ma v ZhETF **5**, 157 (1967) [Sov. Phys.–JETP Letters **5**, 126 (1967)]; Can. J. Phys. **46**, S241 (1968).
12. P. R. Barker, W. E. Hazen, and A. Z. Hendel, Phys. Rev. Lett. **18**, 51 (1967); W. E. Hazen, *et al.*, *ibid.* **22**, 35 (1969); **24**, 476 (1970).
13. V. B. Atrashkevich *et al.*, Yad. Fiz. **28**, 366 (1978).
14. A. Borione *et al.*, Nucl. Instrum. Meth. A **346**, 329 (1994).
15. K. Kadota *et al.*, Proc. 23rd International Conference on Cosmic Rays (ICRC-23), Calgary, 1993, v. 4, p. 262; Tokyo Workshop on Techniques for the Study of Extremely High Energy Cosmic Rays, Tanashi, Tokyo, 27 – 30 Sept. 1993.
16. P. I. Golubnichii, A. D. Filonenko, and V. I. Yakovlev, Izv. Akad. Nauk **58**, 45 (1994).
17. C. Castagnoli *et al.*, Proc. ICRC-23, Calgary, 1993, v. 4, p. 258.
18. R. Baishya *et al.*, Proc. ICRC-23, Calgary, 1993, V. 4, p. 266; Gauhati University Collaboration, paper submitted to this conference.
19. M. A. Lawrence, R. J. O. Reid, and A. A. Watson, J. Phys. G **17**, 733 (1991).
20. R. Gall and K. D. Green, UMC-CASA note, Aug. 23, 1996 (unpublished).
21. D. F. Sullivan, Master's Thesis, University of Chicago, 1999 (unpublished).
22. P. W. Gorham, "On the possibility of radar echo detection of ultra-high energy cosmic ray- and neutrino-induced extensive air showers," hep-ex/0001041, January, 2000 (unpublished).
23. E. Zas, this conference.